International Journal of Automotive Technology, Vol. 6, No. 1, pp. 1−8 (2005)

1229−9138/2005/019−01

EFFECT OF INTAKE PORT GEOMETRY ON THE IN-CYLINDER FLOW CHARACTERISTICS IN A HIGH SPEED D.I. DIESEL ENGINE

K. H. LEE[1)*], J. D. RYU[2)], C. S. LEE[3)] and R. D. REITZ[4)]

[1)]Department of Mechanical Engineering, Hanyang University, Gyeonggi 425-791, Korea
[2)]Graduate School of Hanyang University, Seoul 133-791, Korea
[3)]Department of Mechanical Engineering, Hanyang University, Seoul 133-791, Korea
[4)]Engine Research Center, University of Wisconsin-Madison, 1500 Engineering Drive, Madison, WI 53706, USA

(Received 22 September 2003; Revised 5 July 2004)

ABSTRACT−Recently, the HSDI (High Speed Direct Injection) diesel engine has been spotlighted as a next generation engine because it has a good potential for high thermal efficiency and fuel economy. This study was carried out to investigate the in-cylinder flow characteristics generated in a HSDI diesel engine with a 4-valve type cylinder head. The four kinds of cylinder head were manufactured to elucidate the effect of intake port geometry on the in-cylinder flow characteristics. The steady flow characteristics such as coefficient of flow rate (C_f), swirl ratio (Rs), and mass flow rate (m_s) were measured by the steady flow test rig and the unsteady flow velocity within a cylinder was measured by PIV. In addition, the in-cylinder flow patterns were visualized by the visualization experiment and these results were compared with simulation results calculated by the commercial CFD code. The steady flow test results indicated that the mass flow rate of the cylinder head with a short distance between the two intake ports is 13% more than that of the other head. However, the non-dimensional swirl ratio is decreased by approximately 15%. As a result of in-cylinder flow characteristics obtained by PIV and CFD calculation, we found that the swirl center was eccentric from the cylinder center and the position of swirl center was changed with crank angle. As the piston moves to near the TDC, the swirl center corresponded to the cylinder center and the velocity distribution became uniform. In addition, the results of the calculation are in good agreement with the experimental results.

KEY WORDS : Helical intake port, ISM (impulse swirl meter), Swirl ratio, Intake flow rate, PIV (particle image velocimetry), HSDI (high speed direct injection)

1. INTRODUCTION

As the environmental problems caused by vehicle exhaust emissions become more severe, exhaust emission standards and fuel economy regulations become more stringent. Therefore, efforts to improve the thermal efficiency and reduce the emissions of internal combustion engines are being continued around the world to meet the stringent demands for the prevention of global warming and air pollution. The direct injection (DI) diesel engine has become a prime candidate for future transportation needs because of its high thermal efficiency. Recently, the high speed direct injection (HSDI) diesel engines with single cylinder displacements of 0.5−0.65 liters are being spotlighted to improve the efficiency of small automotive engines. (Noboru, 1997; Herrmann and Durnhoz, 1995) It is well known that this engine generates a large amount of NOx and soot because of locally excessive richness and overall lean combustion. Therefore, a lot of research was conducted to reduce NOx and soot exhausted from the HSDI diesel engines simultaneously. Recently, many papers reported the fact that fuel economy and exhaust emissions of an HSDI diesel engine were improved significantly by using high pressure injection. However, it will not be easy to reach these low emission levels for HSDI engines because it is difficult to form a good mixture formation within the cylinder. In the case of small size high speed diesel engines, a high pressure injection tends to make the injected fuel impinge on the cylinder liner because this kind of injector has a large penetration length. The impinged fuel forms a liquid film and makes an incomplete mixture formation in a cylinder. Thus, technology for enhancing the mixing process is needed to prevent this occurrence. It is well known that the swirl flow generated by intake port is a very useful method to increase the mixing rate. Therefore, a proper understanding of in-cylinder air motion and the design parameters of intake port geometry that can generate an optimal flow pattern are required to form the appropriate mixture formation.

**Corresponding author.* e-mail: hylee@hanyang.ac.kr

In addition, demands for a 4-valve type cylinder head have increased because this 4-valve concept has good potential for a large intake air flow rate and the central location of the fuel injector. Since a large intake flow rate has a great effect on the engine power and because central location of the injector improves combustion efficiency by making air-fuel distribution uniform in the combustion chamber, the design technique for a 4 valve cylinder head is very important in developing an HSDI diesel engine. Therefore, experimental data about the flow field and design parameters of intake port geometry are needed to understand the in-cylinder flow pattern and also to provide the design criteria for the actual HSDI diesel engine development. The flow characteristics of a 2-valve cylinder head with a helical port have been studied for decades by many researchers. The flow characteristics of a 2-valve cylinder head are known to be very different from that of a 4-valve cylinder head. These research are focused on the swirl ratio measured in the steady state condition that is very far from the engine-like condition (Jun-ichi et al., 1998). The experimental results of the steady state condition are also known to be different from the case of the unsteady flow field. Thus, the analysis on unsteady flow characteristics for a 4-valve cylinder head is indispensable. Furthermore, the research that investigates the relation between intake port geometry and flow pattern are very rare.

To overcome some of these limitations, in this paper, various experimental techniques were constructed to measure the flow characteristics and various intake ports were designed to establish the design parameter. The numerical simulation was also conducted to predict the in-cylinder flow field. Steady state flow tests were performed to investigate the intake flow rate and swirl ratio by an impulse swirl meter. On the other hand, unsteady velocity distributions with a crank angle were measured to clarify the swirl generation process by using PIV and visualization single cylinder engine. In addition, a flow visualization test was performed in order to compare the flow pattern between two port geometries by using a laser sheet method and these experimental results were used to validate the CFD calculation results. The purpose of the study was to explore the effect of intake port geometry on the in-cylinder flow characteristics such as swirl ratio, intake flow rate, flow pattern and velocity and also to provide the design parameter of intake port geometry for an HSDI small bore diesel engine.

2. EXPERIMENTAL APPARATUS AND ANALYTIC PROCEDURE

2.1. Intake Port Geometry and Design Parameter of the Test Engine

In this study, the small size direct injection diesel engine with a 4 valve type cylinder head was manufactured to conduct experimental and analytical research. Figure 1 shows the geometry of the intake port and specifications of the test cylinder head are shown in Table 1. The combustion chamber diameter was chosen as 80mm based on the 1500cc engine class. This head has two independent ports, one of them is the helical port to generate a swirl flow and the other is the tangential port to improve an intake flow rate.

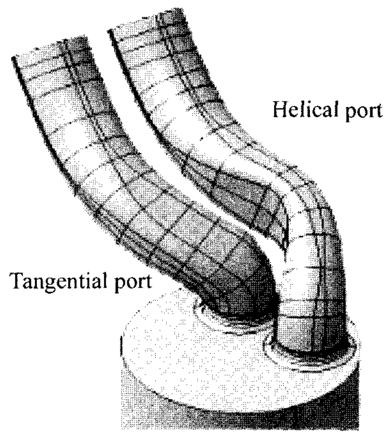

Figure 1. Detail of the intake port geometry.

Table 1. Specification of test cylinder head.

Number of intake valves	2
Cylinder bore	80 mm
Intake valve diameter	24.4 mm
Valve seat angle	45 deg
Distance between each intake valve	31.62 mm

It is known that there are a lot of design parameters for the intake port which affects intake flow rate and swirl ratio (Heywood, 2002). Among these parameters, the protrusions of the valve guide and the distance between two independent intake ports were selected as experimental parameters because these factors have a dominant effect on the intake flow rate and the swirl flow. To investigate the influence of the design parameter on the intake flow rate and swirl generation, we varied the valve guide length to three types (2, 7, 11 mm) and the distance

Table 2. Design parameter of test cylinder head.

Head type	Protrusions of valve guide & guide boss	Distance between each independent port
A-type	7 mm	37 mm
B-type	2 mm	37 mm
C-type	11 mm	37 mm
D-type	7 mm	47 mm

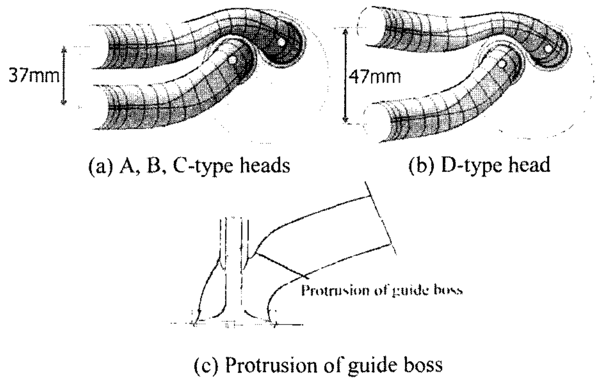

Figure 2. Configuration of test intake ports.

between the two independent ports was changed to two types (37 mm, 47 mm). The design parameters of the test cylinder head are shown in Table 2 and Figure 2 shows the intake port geometries of each cylinder head.

2.2. Experimental Apparatus for Steady Flow Test

The measurement of the intake flow rate and swirl ratio under a steady state condition is important because these factors have a great effect on engine power and combustion, respectively. Figure 3 shows the schematic diagram of the steady state test rig used in this study. This experimental rig was manufactured in order to simulate the intake stroke of real engine operation. During the experiment, the pressure difference between the cylinder head and atmosphere was controlled to be uniform (300 mmAq). The intake flow rate was measured by orifice and the swirl ratio was detected by using an impulse swirl meter. The impulse swirl meter constructed of a honeycomb disk absorbs the angular momentum of the vortex produced by the intake flow. We obtained the swirl ratio from the angular momentum measured by this honeycomb disk (Lee *et al.*, 2002).

2.3. Experimental Apparatus for Flow Field

2.3.1. Flow visualization in steady state condition

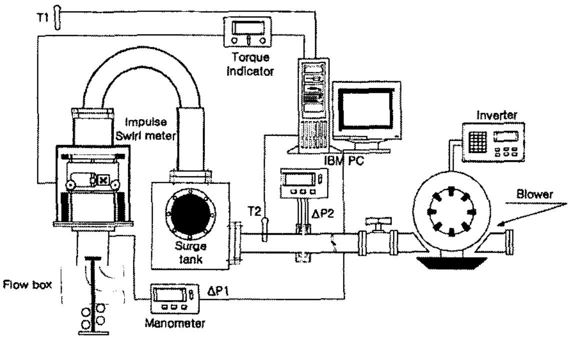

Figure 3. Schematic diagram of steady state test rig.

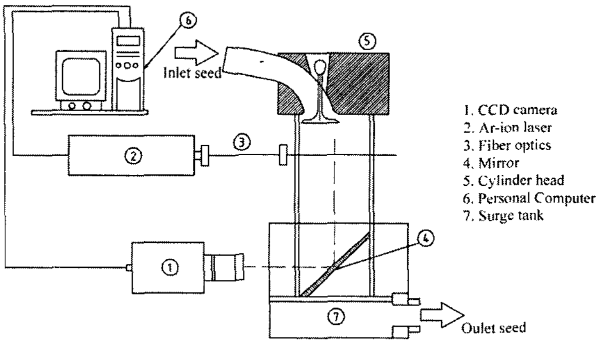

Figure 4. Schematic diagram of visualization system for steady state condition.

The flow visualization experiment in steady state was conducted to observe a qualitative in-cylinder flow pattern that was produced by various intake port geometries. The result of the flow visualization was used to validate intake flow rate and non-dimensional swirl ratio under the steady state condition. In addition, this visualization result helped us to understand the flow pattern produced in the cylinder during intake stroke.

Figure 4 shows the schematic diagram of the flow visualization system. A water-cooled multi-line 5W argon ion laser (LEXEL Co) was used as a source of light. A sheet beam was formed by the optic fiber with cylindrical lens and focused on the testing area. Micro-balloons (with a specific gravity of 3.085 and diameter of 80 μm) were used as scattering particles. The CCD camera (Megaplus ES1.0, resolution: 1018 x 1008, Kodak Co.) took images with an exposure time of 1/30 second.

2.3.2. PIV system in unsteady state condition

The optical engine with a single cylinder was used to measure the in-cylinder velocity by the PIV technique under an unsteady condition. The optical engine was composed of four components such as optical window, elongation piston, extended cylinder block and DC motor. The specification of the optical engine system is shown in Table 3.

Since many diesel engines adopted bowl-in-piston as a combustion chamber shape, flow characteristics within

Table 3. Specification of the optical single cylinder engine.

Engine type	D.I. diesel singe cyl.	Displacement volume	432
Combustion chamber	Bowl-in-piston	Compression ratio	17.5
Bore × Stroke	80 mm × 86 mm	No. of intake valves	2

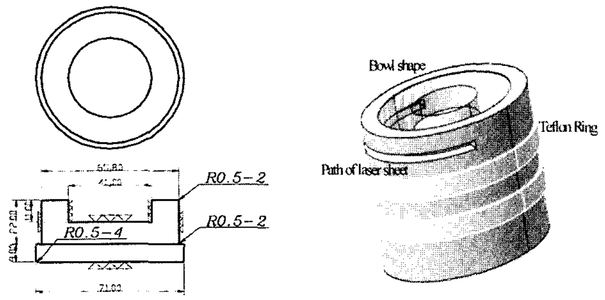

(a) (b)

Figure 5. Detail shape of bowl-in-piston with optical window.

this area have a great effect on engine combustion. In order to measure the flow pattern in the piston bowl, we designed the bowl-in-piston that has an optical window to induce the laser sheet beam. Figure 5 shows the bowl-in-piston shape with optical window. The test area of the combustion chamber is located at 2 mm from the bowl bottom and the material of the optical window installed to piston is quartz.

A PIV system was established to measure the swirl velocity generated in the cylinder during the compression stroke. This system is shown in Figure 6. The Nd:YAG laser (250 mJ, 532 nm) was used as a light source. It generates a laser beam two times sequentially with a short time interval by using a Q switching option. The laser beam passes through the cylindrical lens and is introduced to the observation area in a sheet form with the thickness of 1 mm. The exposure times of the CCD camera and laser beam are controlled by a timing board (PC-TIO-10) and the LabView program. The image obtained by a high resolution CCD camera (Megaplus ES 1.0) is recorded in digital form by an image board. This

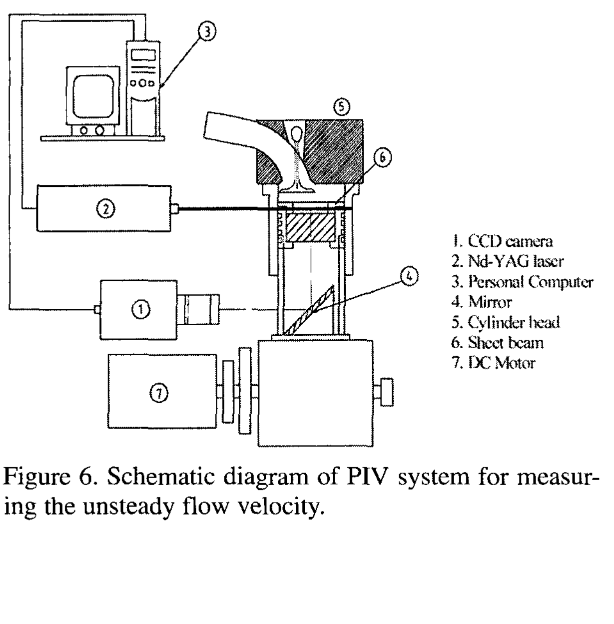

Figure 6. Schematic diagram of PIV system for measuring the unsteady flow velocity.

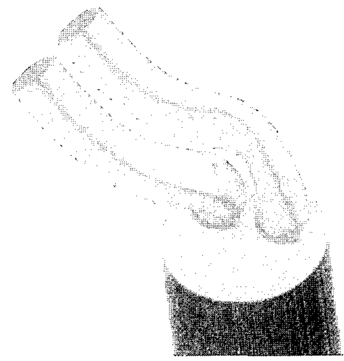

Figure 7. Computational mesh of intake port.

PIV system recorded particle images exposed by each sequential laser beam in separate frames by using a frame straddling method and calculated the velocity vector by a cross-correlation PIV algorithm, which is programmed to obtain the velocity by calculating the coordinates of the location of the maximum cross-correlation parameter.

2.4. Three Dimensional In-Cylinder Simulation

In order to analyze the effects of the intake port geometry on the flow characteristics, it is necessary to investigate the flow field within the intake port and cylinder during the intake stroke. Therefore, three dimensional flow simulations were conducted to predict the flow pattern generated in the cylinder. Three dimensional surfaces for various intake port types were produced by a commercial CAD program called as CATIA. In addition, the grid generation and CFD calculation were conducted by a commercial CFD code(VECTIS). The mesh structure used in this paper was the Cartesian mesh structure and the total number of mesh came to almost 60,000. The procedure of the computational mesh generation for the intake port is shown in Figure 7.

The three dimensional steady state analyses was performed by solving the three momentum equations such as continuity equation, energy equation and k-ε model for turbulence. To compare this model with the experimental result, a pressure-pressure boundary condition was used as the boundary condition. Atmosphere was used as the inlet condition and 300 mmAq was used as the pressure difference between inlet and outlet conditions. The intake flow rate and flow coefficient obtained from the experiment were compared with simulation results in order to validate the simulation results.

3. RESULT AND DISCUSSION

3.1. Intake Flow Characteristics with Intake Port Geometry

Figure 8 shows the comparison of the flow coefficient between four different intake port geometries. The value

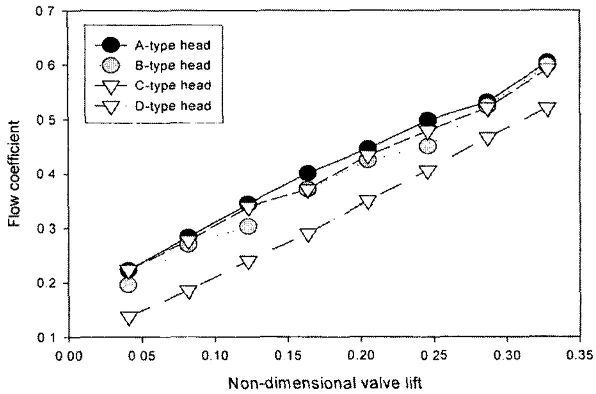

Figure 8. Flow coefficient of intake port with a non-dimensional valve lift.

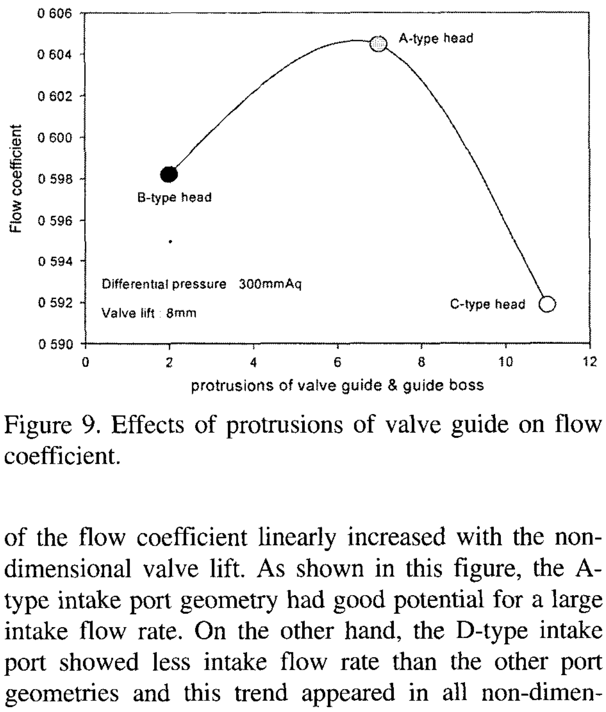

Figure 9. Effects of protrusions of valve guide on flow coefficient.

of the flow coefficient linearly increased with the non-dimensional valve lift. As shown in this figure, the A-type intake port geometry had good potential for a large intake flow rate. On the other hand, the D-type intake port showed less intake flow rate than the other port geometries and this trend appeared in all non-dimensional valve lift regions. In addition, we found that the C-type port had an advantage for intake flow rate at the low valve lift region. From these results, we found that the intake port geometry has a great effect on the intake flow rate and the effect of distance between two ports is larger than that of the protrusion of the valve guide. To select a design guide for a protrusion of the valve guide, the effect of this factor on the flow coefficient was compared with three cases. The experimental results are shown in Figure 9. As shown in this figure, the effects of protrusion on flow coefficient are different according to their length. These results revealed that the large protrusion length disturbed the intake flow rate and 7 mm was chosen as the optimal protrusion length of the valve guide for this test cylinder head.

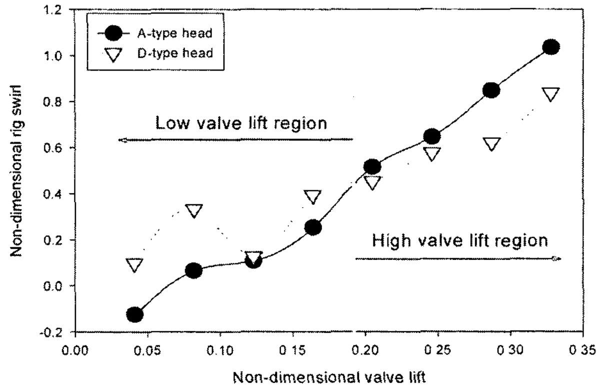

Figure 10. Comparison of non-dimensional rig swirl with valve lift.

Figure 10 shows the non-dimensional swirl ratio with valve lift between two types of cylinder heads. In the case of the low valve lift region, the swirl ratio of the D-type cylinder head is larger than that of the A-type cylinder head. On the other hand, in the case of a high valve lift region, the swirl ratio of the A-type head is larger than that of the D-type head. In order to make clear the reason why this opposite trend occurred, the flow visualization experiment was conducted.

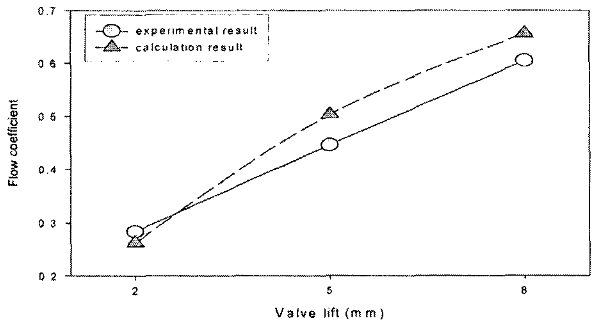

(a) A-type head

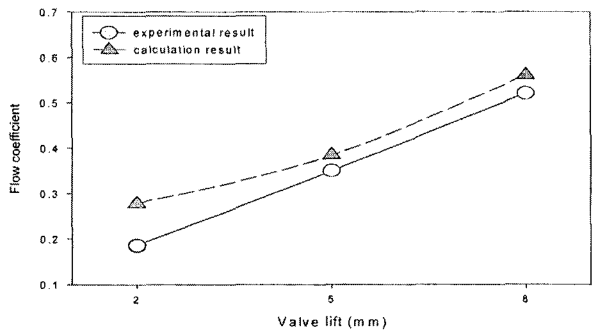

(b) D-type head

Figure 11. Comparison of flow coefficient by calculation and experiment between two cylinder heads.

3.2. Comparison of Flow Coefficient between Two Cylinder Head Types

The flow coefficients of two cylinder heads (A and D types) obtained by experiment and calculation were shown in Figure 11. The flow coefficient linearly increased with valve lift in both cylinder heads. In particular, the increasing rate of the A-type head is larger than that of the D-type head. In addition, the experimental result showed a good agreement with calculation results within 8%. From this figure, we found that the CFD calculation is a very effective tool for predicting intake flow characteristics.

3.3. Comparison of Flow Patterns between two Cylinder Head Types

The calculation results of flow pattern in two cylinder heads (A and D types) were compared with the experimental results in the low and high valve lift cases. The comparison of these results was shown in Figure 12. In the case of low valve lift (Figure 12(a), (c)), two small scale vortices are generated by the intake flow in both cylinder heads. One of the vortices is in a counterclockwise direction and the other is in a clockwise direction. From this figure, we found that two intake flows induced from A-type heads were impinged near the cylinder wall because the distance between the two intake ports is close. Since this impinged flows interrupted the swirl generation, the swirl ratio of the A-type head might be less than that of the D-type head. This result showed good agreement with the steady state test result as shown in Figure 10. In the case of the low valve lift, we found that the swirl flow generated by helical port didn't so fully develop as to dominate another flow generated by a tangential port. On the contrary, in the case of high valve lift, one large swirl flow induced from the helical port is dominated because this flow had enough momentum to overwhelm the other flow induced from the tangential port. This swirl size was similar to the cylinder diameter. However, the swirl flow of the D-type head was smaller than that of the A-type head because the intake flow induced from the tangential port interrupted the swirl generation produced by the helical port. Since there is a large space between the two intake ports in the A-type head, the intake flow induced from each intake port impinged on each other in this space. This result is also in good agreement with steady state experimental results. Therefore, we found that the visualization experiment is a very useful tool for validating the steady flow test results. As valve lift increases, two small size vortices change to one big size vortex which is almost the same as the cylinder bore and the center of the swirl moves to the center of the cylinder. In addition, the flow patterns obtained by calculation showed a similar trend to those of the experimental results.

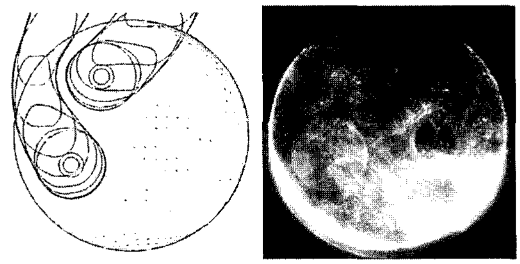

(a) A-type (lift=2mm)

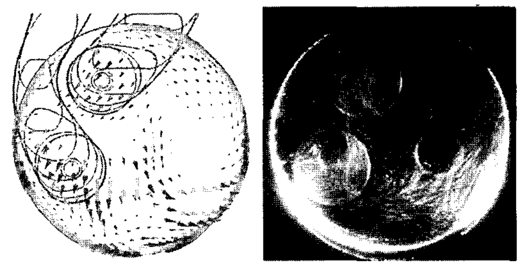

(b) A-type (lift=8mm)

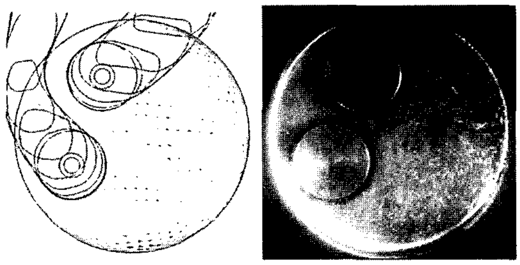

(c) D-type (lift=2mm)

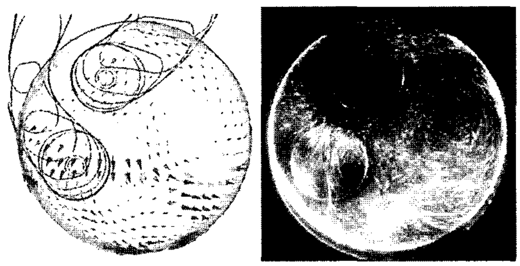

(d) D-type (lift=8mm)

Figure 12. Comparison of flow fields obtained by calculation and experiment between two cylinder heads.

3.4. Velocity Distribution within the Bowl-in-Piston with Crank Angle

Figure 13 shows the test section used to PIV measurement and the area of this test section was 27 mm × 27 mm within bowl-in-piston.

The velocity distributions and velocity contours measured by PIV during the compression stroke are shown in Figures 14, 15 and 16. As shown in these results, the relatively high velocity zone appeared in the outer wall zone of the piston bowl and as the crank angle closes to near the TDC, this strong velocity profile moves in a

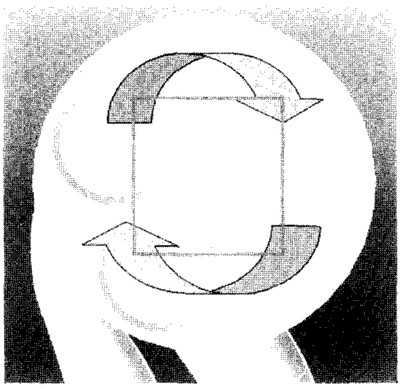

Figure 13. Test section of bowl-in-piston.

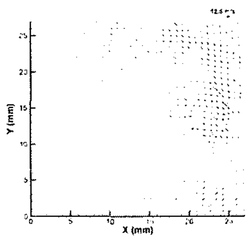

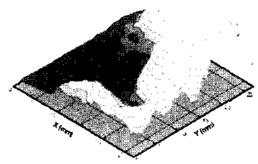

(a) Velocity distribution (b) Velocity contour

Figure 14. Flow field at BTDC 120°.

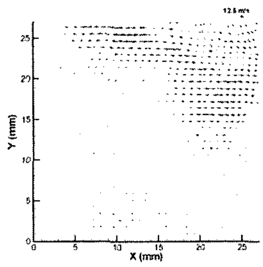

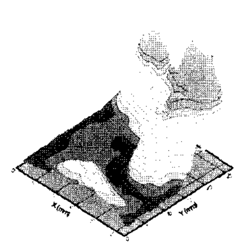

(a) Velocity distribution (b) Velocity contour

Figure 15. Flow field at BTDC 90°.

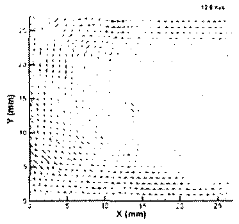

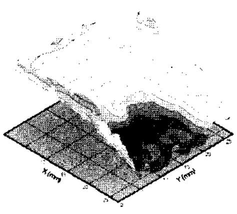

(a) Velocity distribution (b) Velocity contour

Figure 16. Flow field at BTDC 45°.

counter-clockwise direction and generates a swirl flow in the bowl-in-piston. This figure shows that the swirl flow was generated in the piston bowl during the compression stroke and the flow distribution became uniform near the

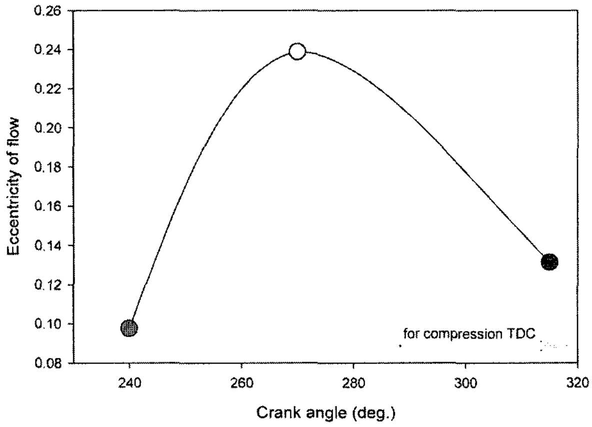

Figure 17. Eccentricity of swirl center.

end of the compression stroke. The results of this research are in good agreement with the other results (Akira *et al.*, 1988; Arcoumnis *et al.*, 1983).

In the BTDC 120 deg, which is the time of the intake valve closing (in Figure 14), the value of the velocity magnitude was lowest and the maximum velocity profile appeared near the exhaust valve. As shown in Figure 15, after closing the intake valve, the maximum velocity profile also appeared near the exhaust valve same as in the case of BTDC 120 deg, but the velocity magnitude was increased. The reason for this development is that as the piston moves upward, velocity magnitude and swirl energy in the bowl zone is increased because the squish flow, which flows from the squish area to piston bowl, strengthened. At the BTDC 45 deg (Figure 16), a large velocity magnitude is observed around the outer wall in the bowl and almost all the velocity magnitude was decreased, compared with the BTDC 90 deg. This result is caused by a decrease of angular momentum. As the piston moves to near the TDC, momentum change occurred by a mass transfer between the squish zone and bowl zone and friction loss is increased. Therefore, the angular momentum is decreased at this crank angle.

Figure 17 shows the eccentricity of the swirl center under an unsteady state condition. These results are calculated by using PIV data. The eccentricity of the swirl center is defined to a non-dimensional distance from cylinder center to swirl center as cylinder bore. Therefore, if eccentricity of the swirl center is "0", this means that the position of the swirl center corresponds to the location of the cylinder center. From this figure, we found that the swirl center changed with the crank angle. In the beginning of the compression stroke (BTDC 120 deg), the eccentricity of the swirl center had a low value and the swirl center was located at the cylinder center. During the compression stroke, the swirl flow generated in the intake stroke moved to the piston bowl zone at BTDC 90 deg. because the intake air was squeezed by the squish area. The large eccentricity of the swirl center appeared at this crank angle caused by an enhanced swirl flow. At the end of the compression stroke (BTDC 45 deg), the eccentricity of the swirl center lowered in value. Therefore, near the TDC, we predicted that the cylinder center was almost identical to swirl center.

4. CONCLUSIONS

In order to optimize the intake port geometry for a high speed diesel engine, a steady state flow experiment, flow visualization experiment, CFD calculation and unsteady flow velocity measurement by PIV were performed. The following conclusions were obtained from the results and analysis:

(1) The effect of distance between two intake ports on the flow coefficient was larger than that of protrusion of valve guide and effect of protrusion showed different trends with its length. The value of 7 mm should be chosen as the optimal protrusion length of the valve guide.

(2) The intake flow rate of the A-type head with a relatively short distance between two intake ports is about 13% larger than that of other port types and non-dimensional swirl ratios of this port have a good potential at high valve lift region. However, in case of a low valve lift, the swirl ratio of a D-type head with a relatively long distance between the two intake ports is about 15% larger than that of A- type head.

(3) The experimental results of the flow coefficient showed good agreement within 8% with the CFD calculation. It is expected that these results is utilized to useful data to understand the intake flow characteristic.

(4) From the velocity distribution obtained by PIV, a high velocity profile was observed in the outer wall zone of the piston bowl at the beginning of the compression stroke, and then the velocity fluctuation and the eccentricity of swirl center decreased to near the end of compression stroke.

ACKNOWLEDGMENTS–This work was supported by the Korea Research Foundation Grant (KRF-2002-042-D00025).

REFERENCES

Akira, M., Masataka, A. and Hiroyaki, H. (1988). Swirl measurements and modeling in direct injection diesel engines. *SAE Paper No.* 880385.

Arcoumnis, C., Bicen, A. F. and Whitelaw, J. H. (1983). Squish and swirl-squish interaction in motored model engines. *Transaction of ASME*, **105**, 105–112.

Heywood, J. B. (1989). *Internal Combustion Engine Fundamentals*. McGraw-Hill Book Co. New York. 220–230.

Herrmann, H. O. and Durnhoz, M. (1995). Development of a DI-diesel engine with four valves for passenger cars. *SAE Paper No.* 950808.

Jun-ichi, K. Hiroshi, O. and Yoshiyuki, T. (1998). Research on a variable swirl intake port for 4-valve high-speed DI diesel engines. *SAE Paper No.* 982680.

Lee, K., Lee, C. and Joo, Y. (2002). Optimization of the intake port shape for a five-valve gasoline engine. *Proc. Inst Mech. Engrs.*, **215,** Part D, 739–746.

Noboru, H. (1997). A view of the future of automotive diesel engines. *SAE Paper No.* 972682.